JMEPEG (2015) 24:345–352
DOI: 10.1007/s11665-014-1277-0

1059-9495/$19.00

# Hemocompatibility Improvement of Chromium-Bearing Bare-Metal Stent Platform After Magnetoelectropolishing

*Ryszard Rokicki, Waseem Haider, and Shivani Kaushal Maffi*

*(Submitted March 22, 2014; in revised form August 24, 2014; published online October 16, 2014)*

**Research was undertaken to determine the influence of the increased content of chromium in the outermost passive layer of magneto-electrochemically refined Co-Cr alloy L-605 surface on its hemocompatibility. The chemistry, roughness, surface energy, and wettability of conventionally electropolished (EP) and magnetoelectropolished (MEP) samples were studied with x-ray photoelectron spectroscopy (XPS), open circuit potential, atomic force microscopy, and contact angle meter. In vitro hemocompatibility of tested material surfaces was assessed using two important indicators of vascular responses to biomaterial, namely endothelialization and platelets adhesion. The endothelialization was assessed by seeding and incubating samples with human umbilical vein endothelial cells (HUVEC) for 3 days before counting and observing them under a fluorescent microscope. The platelet (rich plasma blood) adhesion and activation test on EP and MEP L-605 alloy surfaces was assessed using a laser scanning confocal microscope. The XPS analysis of MEP samples showed significant enrichment of the passive layer with Cr and O when compared with the EP one. The amount of other elements in the passive layer did not show a significant difference between EP and MEP treatments. The adhesion of HUVEC cells shows remarkable affinity to surfaces enriched in Cr (MEP) with almost 100% confluency. In addition, the number of platelets that adhered to standard EP surfaces was higher compared to the MEP surface. The present study shows that the chromium-enriched surface of cobalt-chromium alloy L-605 by the magnetoelectropolishing process tremendously improves surface hemocompatibility with regard to stent functionality by enhanced endothelialization and lower platelet adhesion and should be taken under consideration as an alternative surface of biodegradable polymer drug-eluting stents, polymer-free drug-eluting stents as well as bare-metal stents.**

**Keywords** biomaterial, magnetic, magnets, oxidation, stainless, steel

## 1. Introduction

The primary goal of the introduction of drug-eluting stents (DES) was to cut the high restenosis rate of bare-metal stents (BMS) and thus reducing the need of repeated revascularization. However, shortly after their introduction, unexpected but very significant problem has appeared, namely, an increased rate of thrombosis with very dangerous consequences. In response to this, the Food and Drug Administration (FDA) issued the guideline for the need of dual antiplatelet therapy (DAPT) up to 12 months after implantation of DES (Ref 1). The second generation of DES introduced several changes compared to the previous one: new more fatigue-resistant alloys (cobalt-chromium and platinum-chromium) which consequently allowed utilization of a thinner strut, more biocompatible and thinner polymers, and new immunosuppressant drugs such as everolimus and zotarolimus. These changes showed overall improvement over the first generation, but they are still not able to totally eliminate late events and shorten the duration of dual antiplatelet therapy (DAPT). Looking for the culprit responsible for this, Waksman (Ref 2) points again to polymer as was in the case of first generation DES. The solution to the problems associated with the durable polymer DES (first as well as second generation) has been the widespread development of the biodegradable polymer drug-eluting stent (BPDES).

Theoretically the new, but not totally new, concept of BPDES looks very promising. However, its precursor, namely NEVO-Cordis-J&J BPDES, did not succeed (Ref 3). The main difference between NEVO and the present generation of BPDES are the places from which the drug is released. In the case of NEVO, the drug was released from biodegradable polymer confined in the reservoirs situated in the struts of the stent. Contemporary BPDES releases the drug from the polymer which covers the abluminal stent surface. The main similarity of whose stents are their unmodified bare metal surface. Unfortunately, the latest studies by Christiansen et al. (Ref 4), Smith et al. (Ref 5), and Tada et al. (Ref 6) do not show overwhelming differences regarding the primary end point of biodegradable polymer versus durable polymer DES. This time, the suspected culprit is unquestionably the bare-metal stent surface itself after the drug is eluted and biodegradable polymer is gone. Due to their high strength, toughness, elasticity, and corrosion resistance, chromium-bearing alloys are extensively used as material for cardiovascular stent platforms. The main contemporary alloys used as cardiovascular stent platforms are stainless steel-316Lvm, Co-Cr-alloy L-605, nickel-cobalt-

**Ryszard Rokicki**, Electrobright, Macungie, PA; **Waseem Haider**, Mechanical Engineering Department, University of Texas-Pan American, Edinburg, TX; and **Shivani Kaushal Maffi**, Department of Molecular Medicine, University of Texas Health Science Center at San Antonio and Edinburg Regional Academic Health Center, Edinburg, TX. Contact e-mail: info@electrobright.com.

chromium-molybdenum alloy MP35N, and newest platinum-chromium alloy Pt-Cr. In all of these alloys, chromium plays the essential role in the corrosion resistance by spontaneously creating the passive layer consisting mainly of $Cr_2O_3$. Unfortunately, this spontaneously formed passive layer is not hemocompatible enough for cardiovascular stents and is prone to thrombosis and restenosis. This inadequacy can be changed by increasing the chromium content in the outermost layer of the chromium-bearing stent. Poperenko et al. (Ref 7) showed that chromium-sputtered stainless steel had thicker chromium oxide $CrO_x$ and a lower adhered platelets count compared to untreated 316 stainless steel, which indicates better thrombo-resistivity. However, the main drawback of such a constructed enriched chromium oxide layer was its impaired corrosion resistance when compared to untreated stainless steel. The impaired corrosion resistance of the passive layer created by this method could consequently lead to harmful metal ions released to the vessel wall and circulating blood which could became the source of chronic inflammation.

The other way to create a corrosion-resistant and simultaneously more hemocompatible and endothelial-friendly surface of chromium-bearing stent platforms is to enrich those surfaces with $Cr_2O_3$ by an electrochemical process, namely magnetoelectropolishing (Ref 8). Our previous work has shown significant chromium enrichment of passive layer of magnetoelectropolished (MEP) 316L ss compared with conventionally electropolished (EP) (Ref 9). The principle of this process is a very strong interaction between externally applied magnetic fields and ferromagnetic elements (Fe, Ni, Co) of anodically dissolved alloy.

The cardiovascular chromium-bearing stents consist of ferromagnetic elements which, during magnetoelectropolishing, are dissolved faster as chromium which is antiferromagnetic and interact very weakly with an applied magnetic field. By this action, the passive layer of MEP chromium-bearing alloy becomes depleted or totally devoid of ferromagnetic elements (Fe, Ni, and Co) and enriched with chromium which spontaneously oxidized upon termination of magnetoelectropolishing process.

By the introduction of abluminally covered BPDES, the stent evolution is coming almost full circle, back to square one: bare metal surfaces. As can be seen, the hemocompatibility problem of BMS reappears and this time demands proper attention and a solution before the BPDES can lead to considerable efficacy improvements over previous ones. Some leading researchers in the stent area predict that BPDES will become the "workhorse" technology for future DES (Ref 10). Stent pioneer Palmaz and other researchers in this field believe that the future of stenting lies in a return to the pure bare-metal stent with a modified surface (Ref 11, 12). But regardless of which technology will take the lead, it is apparent that we never abandoned BMS and we are already starting to return in some instances to bare-metal stent surfaces by introducing BPDES or directly drug-covered stents. It is obvious that to change already known clinical outcomes of BMS, their surfaces have to be altered. As was mentioned, recent studies (Ref 4–6) do not show overwhelming differences regarding the primary end point of BPDES versus durable polymer DES. Also, the COMFORTABLE AMI study (Ref 13) has shown only the superiority of BPDES (BioMatrix) compared with standard BMS. It is worthy of note that in those trials, compliance with dual antiplatelet therapy for up to one year was required which not differed from the guidance for durable polymers DES, but this highly anticipated shorten (DAPT) was not confirmed.

In this study, we undertook the evaluation of magnetoelectropolished surface of one of the chromium-bearing alloys used as cardiovascular stent material, namely Co-Cr alloy L-605 on HUVEC cell and platelets adhesion, proliferation, and aggregation.

## 2. Materials and Methods (Preparation of Samples)

### 2.1 Cutting and Abrasive Polishing

The samples, 10 mm in diameter and 2.5 mm thick, were cut from a Co-Cr alloy L-605 rod which was obtained from Fort Wayne Research Products Corporation (Fort Wayne, IN). After cutting, the samples were successively mechanically polished using grades 400, 600, and 1500 silicon carbide paper and then cleaned ultrasonically in distilled water.

### 2.2 Electropolishing (EP)

The mechanically polished samples underwent an EP process below oxygen evolution regime.

The electrolytic cell for EP consisted of a transparent 500-mL beaker. The L-605 sample was vertically positioned in the center of the beaker about 30 mm below the surface of electrolyte. The cathode consisted of 316L stainless steel screen positioned around the internal beaker wall. The EP was performed for 5 min in room temperature of 25 °C under a constant potential of 10 V. After EP, the samples were ultrasonically cleaned in distilled water.

### 2.3 Magnetoelectropolishing (MEP)

The MEP was performed in identical conditions, as conventional EP process accepts externally applied magnetic field. The magnetic field was imposed on electrochemical system by four ring magnets stacked together with electrochemical cell inside. The magnets were magnetized by their thickness. The imposed magnetic field, around 100 mT, was directed parallel to the electropolished work-piece surface (sample). The Lorenz force effect was observed visually during the MEP process (circular movement of electrolyte around sample).

### 2.4 XPS Study

The chemical composition of the surface layer of differently finished L-605 samples (EP, MEP) was analyzed by x-ray photoelectron spectroscopy K-alpha system (Thermofisher Scientific).

### 2.5 OCP Study

The general corrosion behavior of Co-Cr alloy L-605 in Ringer's solution maintained at 37 °C temperature level was evaluated during 72 h of exposure by the measurement of the open circuit potential (OCP) against Ag/AgCl electrode as a reference. The OCP values were recorded every 1 min during the whole period of exposure and then plotted versus time.

### 2.6 Surface Roughness: Atomic Force Microscopy (AFM)

The roughness measurements were performed by atomic force microscopy. Three scan sizes (2 μm × 2 μm, 10 μm × 10 μm, and 20 μm × 20 μm) were used for both samples.

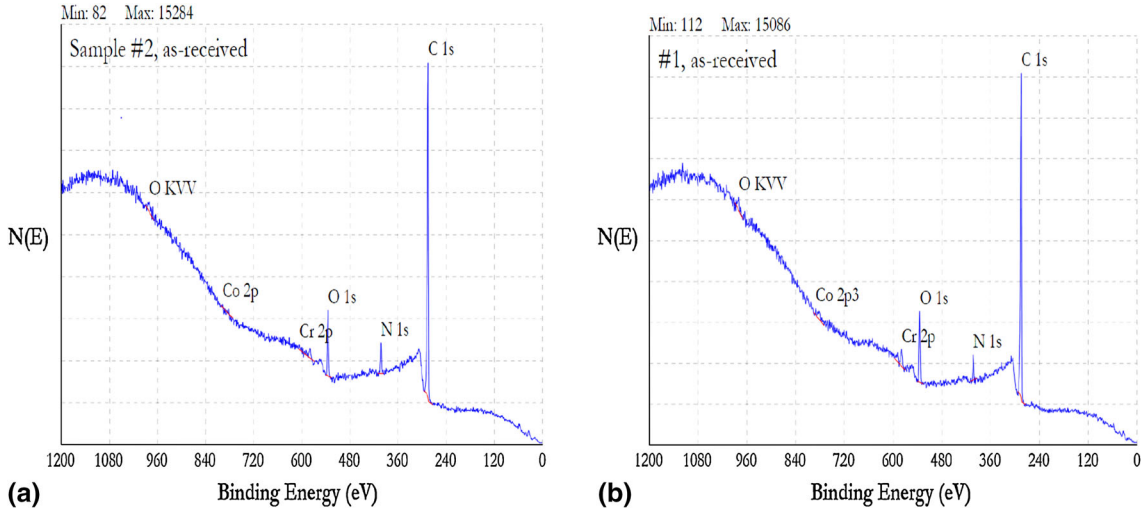


**Fig. 1** XPS survey: (a) EP, (b) MEP

### 2.7 Contact Angle Measurement

The wettability contact angle was measured by sessile drop method using Kyowa contact angle meter (DM-CE1, Kyowa, Japan).

### 2.8 In Vitro HUVEC Cell-Biomaterial Interaction

The growth of HUVEC cells on the surface of Co-Cr alloy L-605 was assessed using the ISO 10993 protocols for biological evaluation of medical devices. This was accomplished by using an Olympus IX81 fluorescent microscope to take images. HUVEC cells were maintained in accordance with the instructions provided by the commercial source (American Type Culture Collection, ATCC). The cells were first cultured in a 75-$cm^2$ cell culture flask using F-12K as the medium. When confluency was achieved by the cells, they were trypsinized, centrifuged, and re-suspended in culture media for cell counting and cell seeding.

In order to assess the endothelial cell proliferation, Co-Cr alloy L-605 samples, 10 mm in diameter, were placed into a 24-well plate and seeded with $50\times10^3$ cells per well. Cell culture plates with Co-Cr alloy L-605 were incubated for 72 h at 37 °C, 5% $CO_2$ in cell culture media. Later, cell culture media were removed and samples were gently washed with DPBS. Two mL of Hoechst dye (5 μM) and Mitotracker Red dye (100 nM) were added into the wells. Hoechst dye was used to highlight the nuclei of the cells, while Mitotracker Red dye was used to highlight the mitochondria of the cells. The plates were again incubated for 20 min, after which the Co-Cr alloy L-605 samples were washed 3 times with DPBS. Finally, the cells were fixed on the surface of the alloys with 10% formaldehyde and covered by glass slides. Cells were counted by randomly choosing an area of 400 $\mu m^2$. The consistency of the result was ascertained by performing experiments at least three times.

### 2.9 In Vitro Blood Platelets: Biomaterial Interaction

Platelet-rich plasma (PRP) was purchased from Zen-Bio, Inc. Research Triangle Park, NC, USA and used immediately upon arrival. The concentration of the PRP was adjusted to $1 \times 10^5/\mu L$ with Tyrode's buffer pH 7.4 (134 mM sodium chloride, 12 mM sodium bicarbonate, 2.9 mM potassium chloride, 0.34 mM sodium phosphate monobasic, 5 mM HEPES, and 5 mM glucose). Before the start of experiment, platelets were acclimatized by adding 1 mL of PRP to Nunc cover glass chambers and incubating for 1 h. To identify entire cellular morphology, cells were then loaded with 5 μM Oregon green 488 carboxylic acid diacetate (DFFDA) (Life Technologies) for an additional 30 min at 37 °C. In a separate culture dish, Co-Cr alloy L-605 samples were warmed in the incubator all along. The samples were then transferred to the Nunc chambers for 5 or 30 min. Thereafter, the PRP was substituted with Tyrode buffer to remove all unbound cells. The metal alloys were flipped to expose the bound cells toward the microscope objective. Images of the adherent platelets were captured immediately using an Olympus FV1000 confocal microscope equipped with a 60× objective, NA 1.42, using standard 488-nm Argon laser settings with excitation/emission of (488/520 nm). Laser intensity output and scan speed (8 μs/pixel) for image acquisition were attenuated to minimize photo-bleaching and photo-toxicity. Five-six images per sample were randomly obtained from each group to determine platelet number, morphology, and activation

## 3. Results

### 3.1 XPS Survey and Chemical Data

Figure 1 presents XPS survey of Co-Cr alloy L-605 after consecutive treatments: Fig. 1a—EP, Fig. 1b—MEP.

ESCA data of varying concentration of C, Co, Cr, Ni, W, and O are shown in Table 1. It is clearly seen that MEP treatment has enriched passive oxide layer in Cr. The atomic concentration of chromium increased to about 30% after MEP when compared to the EP sample. The Ni and W were not detected in passive layers of either sample. Co has shown small increase in MEP sample. MEP sample also shows 10% higher concentration of oxygen compared to EP.

### 3.2 Open Circuit Potential

The open circuit potential results of Co-Cr alloy L605 EP and MEP samples in the Ringer's solution are presented in (Fig. 2). One can easily notice the shifting of OCP of sample

**Table 1 Elemental concentration of Co-Cr alloy L-605 oxide layer detected using XPS**

| Sample | Elements | | | | |
|---|---|---|---|---|---|
| Co-Cr alloy L-605 | Co | Cr | Ni | O | W |
| EP | 0.4 | 1.1 | ND | 7.8 | ND |
| MEP | 0.5 | 1.5 | ND | 8.7 | ND |

ND: None detected

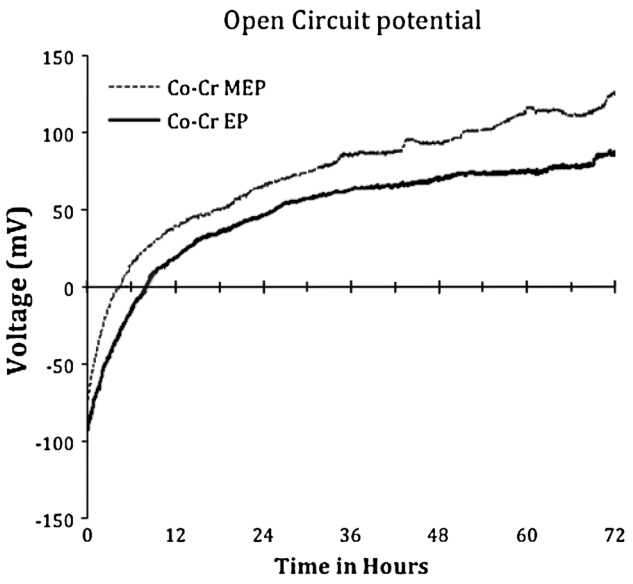


**Fig. 2** Open circuit potential of EP and MEP Co-Cr alloy L-605 in Ringer's solution as a function of the immersion time

**Table 2 Ra of Co-Cr alloy L-605 after EP and MEP**

| Magnitude | scan size, μm | | |
|---|---|---|---|
| Co-Cr alloy L-605 | 2 × 2 | 10 × 10 | 20 × 20 |
| Ra, μm EP surface | 0.646 | 2.595 | 6.073 |
| Ra, μm MEP surface | 0.57 | 2.339 | 5.872 |

$n = 3$

surface after MEP in more positive direction in comparison with the results obtained after EP treatment. Both samples show monotonous increase of OCP with passing time. The shift between the values of OCP of EP and MEP samples stay almost unchanged through the time of experiment (72 h).

### 3.3 Surface Roughness

The results of roughness measurement are shown in Table 2. As can be seen, the roughness of the MEP sample is lower than that of EP for all three taken scan sizes. The differences are not very significant and are in the same value range.

### 3.4 Contact Angle

To evaluate the difference between EP and MEP CO-Cr alloy L-605 wettabilities, the contact angles between L-605 surface and three different liquids were measured. The five readings for every sample were taken, and the average values are presented in Table 3. As could be expected, the MEP sample surface showed a lower water contact angle of 70.3° compared to 77.1° of EP sample.

### 3.5 In Vitro HUVEC Cell-Biomaterial Interaction

The HUVEC cell adhesion and proliferation on EP and MEP Co-Cr alloy L-605 after 72 h of incubation are shown in Fig. 3. The profound difference at qualitative and quantitative levels of HUVEC cell between EP and MEP surfaces is vividly evident. The cells on EP surface differ between each other in shape and size. In some places, they clump up together in bigger agglomerates. On MEP surface, almost all cells look alike and have a very distinctive spindle shape with a very visible pattern of mitochondria on the opposite end of elongated cell divided by centrally situated nucleus. At quantitative level, MEP sample surface reached almost 100% confluency compared to below 50% confluence of EP sample surface. The results of cells counting (average of three samples) are as follows: 10 on the EP sample and 26 on MEP.

### 3.6 In Vitro Platelets-Biomaterial Interaction

The micrographs (Fig. 4) indicate that EP surfaces support a higher number of adhered platelets than MEP surfaces for both times of exposure. The numbers of adhered platelets stay almost unchanged individually for EP as well as MEP surfaces without showing any apparent signs of aggregation with passing time from 5 to 30 min.

## 4. Discussion

Immediately upon introduction of BMS to percutaneous coronary intervention, work was undertaken in the direction to improve their hemocompatibility. The electropolishing process, which has shown to improve stent thromboresistivity and inhibit neointimal hyperplasia to some extent (Ref 14, 15), was adapted without any critical changes and, to these days, is used as a finishing process for almost all BMS.

However, electropolishing was not able to combat the restenosis problem and stents become covered with durable polymers eluting immunosuppressant drugs which inhibit neointimal hyperplasia. But by fixing the problem of restenosis, the durable polymers introduced an even more dangerous problem of thrombosis. The partial answer to this was the introduction of DAPT up to one year after implantation of DES (Ref 1). The next step in stent evolution was the introduction of next generation stents with thinner struts, different immunosuppressant drugs, and more

**Table 3 Wettability components**

| Sample | Contact angle, ° | | | (Interfacial free energy, mJ/m$^2$ | | | Work of adhesion, mJ/m$^2$ | | |
|---|---|---|---|---|---|---|---|---|---|
| Co-Cr alloy l-605 | Water | Ethylene glycol | Diodo-methane | Water | Ethylene glycol | Diodo-methane | Water | Ethylene glycol | Diodo-methane |
| EP | 77.1 | 63.7 | 58.0 | 13.4 | 8.5 | 2.8 | 89.1 | 69.1 | 77.7 |
| MEP | 70.3 | 59. | 55.3 | 6.8 | 6.6 | 2.3 | 97.3 | 72.6 | 79.8 |

$n = 5$

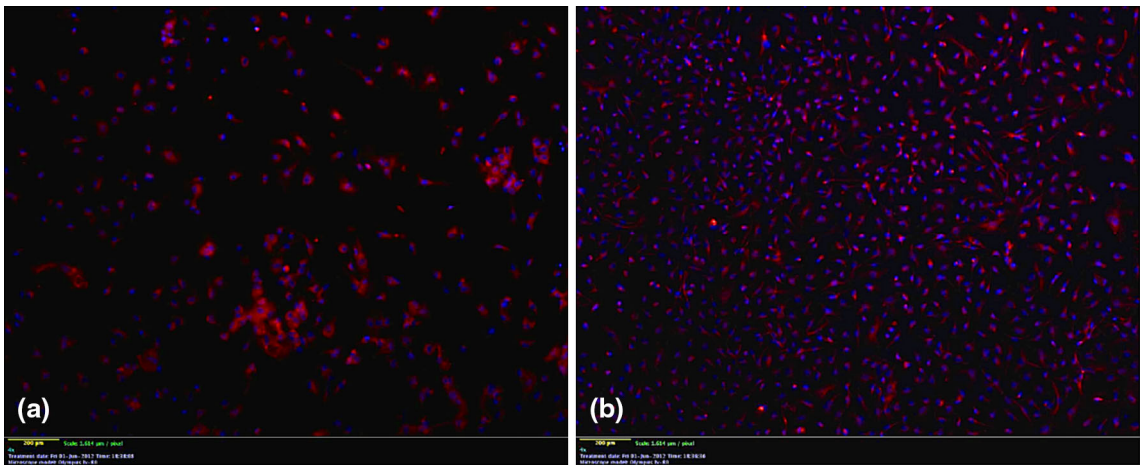


**Fig. 3** Images of HUVEC cells attachment (a) EP and (b) MEP Co-Cr alloy L-605 surfaces after 72 h of incubation

hemocompatible but still durable polymers. They showed improvement over the first generation of DES, but they are still not free from late events. After finding the factor responsible for those events, namely durable polymer, the research became aimed in the direction to eliminate the durable polymer by substituting it by a biodegradable one. However, as was mentioned earlier, the latest studies of BPDES do not show overwhelming differences regarding the primary end points. In our opinion, this is caused by bare-metal stent surface. After the drug is eluted and biodegradable polymer is gone, we can expect exactly the same problems as we have with BMS. In both cases, the stented vessel contacts to some extent the thrombogenic surface. To change this outcome, the bare metal surface has to be more hemocompatible. Peculiarly, only one new process, namely magnetoelectropolishing (Ref 8), was developed for further improvement of metallic stent surface hemocompatibility in the boundary of its own chemical composition.

It is well recognized that blood protein adsorption on the stent surface is a prerequisite of stent-blood cells interaction. After biodegradable polymer is eroded, the bare stent surface is covered by soluble plasma proteins. The proteins adsorption is a dynamic process and depends on many factors such as stent chemical and physical properties, plasma protein concentration, stent and proteins surface electrostatic charge, wettability, hydrophobic interactions, isoelectric points, etc. Despite critical importance of proteins adsorption rates, sequence, amounts, orientation, and conformation on the implanted stent successful integration with blood vessel, it is not possible to exactly predict the stent-proteins in vivo interaction mainly due to the Vroman effect (Ref 16). The Vroman effect postulates constant competition of proteins over binding sites on the surface of biomaterial. The smallest and most abundant protein molecules will adsorb first, but later they are replaced by other ones with highest affinity to particular surface. Albumins, the most abundant blood protein, will adsorb first on negatively charged chromium-bearing stent surfaces in spite of their own negative net charge. This can be explained by charge anisotropy of non-evenly distributed negative and positive charges of functional groups on the surface which only when combine giving total negative net charge to albumin. The electrostatic net attraction will be established by the interaction of negatively charged hydrophilic chromium-bearing stent surfaces and positively charged albumin subdomains. It is also worth to note that proteins with low internal conformational stability (e.g., albumin) tend to adsorb on all surfaces irrespective of electrostatic interactions due to conformational entropy gain upon adsorption (Ref 17). Fibrinogen, a negatively charged blood-clotting protein, also contains substantial hydrophobic and cationic functionality (Ref 18) which allows adsorption to a negatively charged surface. Taking under consideration its major physiological function as the precursor to fibrin and ability to form bridges between platelets by binding to their GpIIb/IIIa surface membranes, fibrinogen adsorption to the stent surface is an unwelcome event because of higher risk of thrombosis.

It is expected that bare-metal stent surfaces upon implantation will be immediately covered by albumin and other abundant transport proteins in regard to their high plasma concentration. This firstly adsorbed layer will undergo replacement by protein of higher affinity to BMS surface, namely fibrinogen. Those processes will have a decisive influence on further stent-cell interaction. Theoretically, albumin will decrease platelet attachment and activation on some surfaces

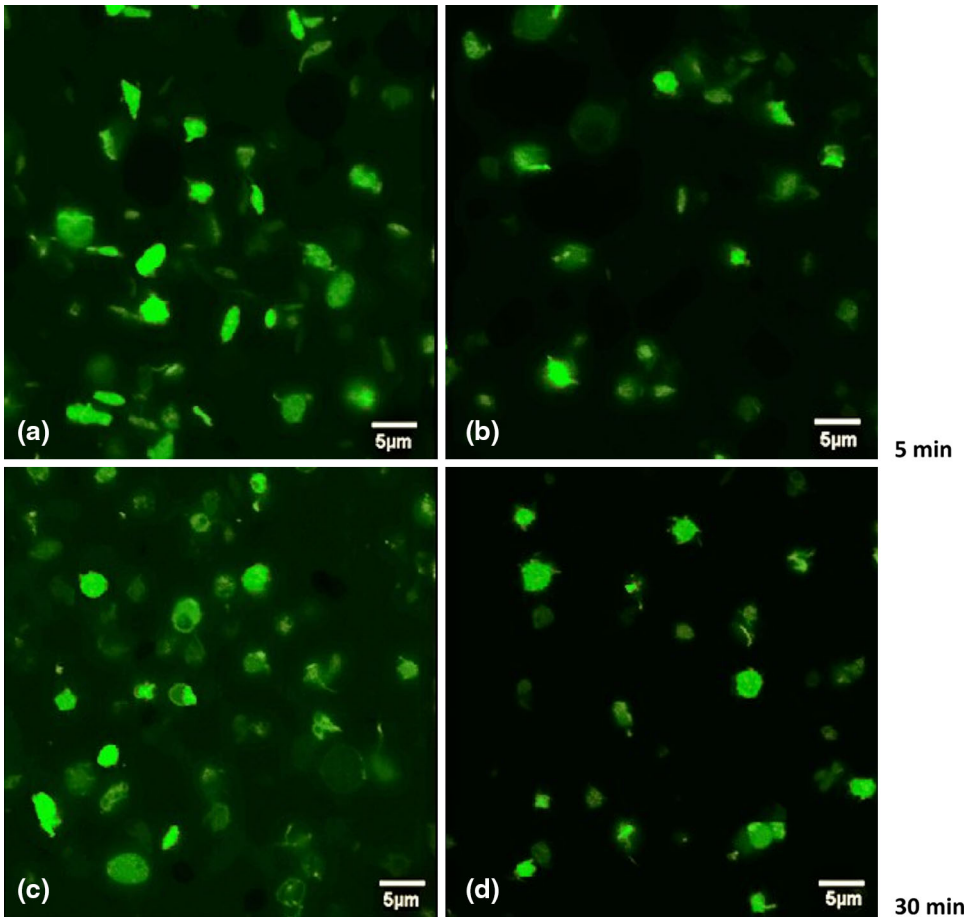


**Fig. 4** Platelets adhesion to Co-Cr alloy L-605 after 5 and 30 min (a, c) EP, (b, d) MEP

but at the same time will decrease the speed of endothelialization, whereas fibrinogen will activate platelets but will accelerate endothelialization (Ref 19). The study of Lambrecht et al. (Ref 20) has shown that an albumin-coated surface bonds less platelets which indicate the importance of the initial interaction between protein and metal surfaces on the process of platelets adhesion and aggregation.

Here comes the necessity of changing the above-mentioned protein adsorption sequential pattern on bare-metal stent surface by changing the chemical composition of passive layer in the more favorable direction to attract and increase albumin adsorption and discourage fibrinogen from binding to the stent surface.

This is done to some extent by electropolishing process as a final finishing step of BMS. Electropolishing action removes native spontaneously formed oxide together with its imperfections and flaws from chromium-bearing stents and creates new more perfect oxide with elevated concentration of chromium in the form of $Cr_2O_3$ (Ref 20) with lower relative permittivity. This new chromium-enriched oxide is not only more corrosion resistant, but also more hemocompatible in regard to stent functionality, namely, it is more thromboresistant and inhibitory to neointimal hyperplasia (Ref 15, 21).

The surface electrostatic force of oxide is one of the factors which influence adsorption of protein as albumin and fibrinogen. Bernabeu et al. (Ref 22) found that negatively charged proteins could be adsorbed onto a negatively charged surface and the adsorption increased with increasing negative surface charge. To increase negative electrostatic force of chromium-bearing stent surface to attract and bind more albumins, its relative permittivity has to be lowered. This is done to some extent by electropolishing, which increases chromium concentration in passive oxide layer, thus increasing the negative electrostatic force but can be pushed even higher by applying magnetoelectropolishing process (Table 1).

The XPS study clearly showed that the sample of Co-Cr alloy L-605, which underwent magnetoelectropolishing treatment, is enriched not only in chromium but also with oxygen (Fig. 1). The adsorption of protein is also influenced by physical properties of the metallic surface, namely roughness which influence total surface area of the samples. The bigger surface area of metallic surface will promote higher density of proteins adsorption. However, in our study, the difference of surface roughness between EP and MEP samples is not big enough (Table 2) to change drastically the surface area of particular samples, and thus it cannot be considered as a primary factor of proteins adsorption.

From a practical point of view, the most important electrochemical parameter characterizing the behavior of metallic material in corrosive liquid environment is open circuit potential (OCP) and particularly its dependence on time of immersion. Both samples of Co-Cr alloy L-605 (EP and MEP) have shown steady monotonous increase of OCP through the duration of the experiment in Ringer's solution. The only

difference between samples was about 30% shift of potential in more positive direction in case of MEP sample which was maintained at almost unchanged level throughout the duration of the experiment (Fig. 2). This phenomenon coincides with an almost identical 30 % increase of Cr content in the outermost passive layer of MEP sample (Table 1). The steady increase of OCP toward more positive values for both samples can be explained by a partial dissolution of $Cr_2O_3$ oxide by Ringer's solution which immediately becomes oxidized to hydrated chromium oxide which is readsorbed on the top of remaining $Cr_2O_3$ oxide. The hydrated chromium oxide undergoes olation (reaction 1) and oxolation (reaction 2) processes which transform chromium oxide passive film in polymeric structure bound by hydroxyl -OH- and oxy-O-bridges.

$$[Cr(OH)6]^{+3} \Leftrightarrow [Cr(H2O)4(OH)2]^{+} + 2H^{+} \rightarrow \text{dimerization} \rightarrow \text{polymerization}$$

(1) (2)

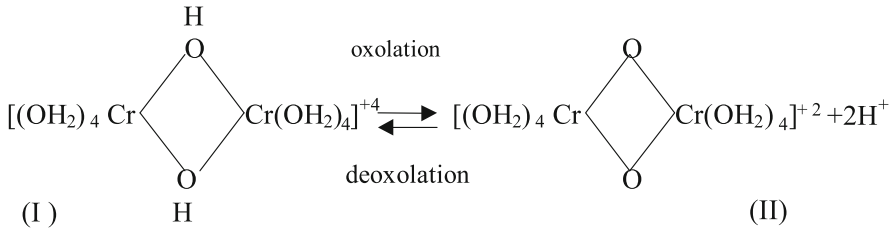


The polymeric chromium oxides are more stable in the presence of $Cl^-$ ions (Ref 23). The higher value of OCP of MEP sample can be explained by the fact that the oxolation is positively driven by an increased amount of $Cr^{3+}$ hydrated ions which is higher on MEP samples. Consequently, the MEP process creates more functional groups ($OH^-$) which are platelets adhesion suppressant (Ref 24). The current results confirmed previous reports of the low affinity of platelets and proteins for hydroxyl group-bearing materials (Ref 25, 26).The increased density of surface hydroxide groups improves hydrophilicity of metallic surface which is regarded to be more hemocompatible. The wettability of both samples remained in high hydrophilic range $\geq 70°$ with no significant differences (Table 3). The process is of paramount importance taking under consideration the paucity of functional group of untreated metallic surface (Ref 27, 28). The study of Martins at el. (Ref 29) suggested that ideal percentage of surface hydroxyl group may increase albumin affinity without fibrinogen adsorption. It is worth noting that reverse process of deoxolation, which can destroy polymeric structure of chromium, is mitigated by almost neutral pH $\approx$ 7.3-7.4 of Ringer's solution and also will be maintained for stent under contact with blood (pH $\approx$ 7.4) upon its implantation.

As we mentioned before, it is no coincidence that all cardiovascular stent platforms are chromium bearing. The ability of chromium to undergo olation (reaction 1) and oxyolation (reaction 2) and stay in this polymeric state in nearly neutral (blood pH $\approx$ 7.4) liquid environment makes chromium-bearing surface very hemocompatible.

As can be seen from micrographs (Fig. 4), the MEP surface shows less adhered platelets compared with EP for both times of exposure. Also after 30 min of incubation, phenotype of platelets stayed almost unchanged without any sign of aggregation. This lower number of total platelets on MEP surface most probably can be attributed to higher density of albumins which adsorb, in bigger amount, on more negative MEP surface. Albumin is considered to be non-adhesive to platelets due to the lack of established domains for platelets bindings (Ref 30). Together, these findings suggest that a MEP stent surface should become more thromboresistant than its EP counterpart.

From endothelialization results of Co-Cr alloy L-605 obtained in our study, we can suspect that a MEP stent platform of BPDES will undergo faster and fuller endothelialization after the erosion of polymer (Fig. 3) and thus decreasing the risk of thrombosis. Theoretically, when a stent undergoes a fast, full, and functional endothelialization, the problems of thrombosis and restenosis should not exist. The spindle shape, same size, visible mitochondria, and nucleus of endothelial cells grown on MEP surface in static condition indicate that endothelial cells did not change their normal phenotype (Fig. 3). Taking under consideration the improved corrosion resistance of MEP surface (Fig. 2) which is inseparable with the decrease of metals cations leaching from stent surface which are the main culprits of inflammatory reaction of tissue surrounding stent struts, the neoatherosclerosis most probably could be prevented or at least minimized for stents which underwent magnetoelectropolishing treatment.

We conclude that the primary factor responsible for those beneficial changes of improved hemocompatibility is the ability of chromium oxide $Cr_2O_3$ to undergo partial dissolution in body fluid (blood) and after immediate hydration, readsorb on top of the remaining chromium oxide and undergo polymerization by olation and oxolation processes. Due to hydroxyl group of polymerized chromium oxide, the surface becomes able to crosslink the protein e.g., albumin friendly to endothelial cell which leads to speedy stent endothelialization.

## 5. Conclusion

Applying the novel magnetoelectropolishing finishing process to biodegradable polymer cardiovascular chromium-bearing stents platforms simultaneously enhances their corrosion resistance and hemocompatibility which is of paramount importance in case of stents functionality. The improved corrosion resistance is due to chromium enrichment of passive layer by the application of a magnetic field during the electropolishing process. The higher amount of chromium (about 30%) in passive layer of MEP surface is responsible for creating more functional hydroxyl groups on the surface of stent by olation and oxolation processes which can crosslink more endothelial cell friendly proteins, e.g., albumins as conventionally EP one and thus making stent more hemocompatible. This study shows that MEP process has all potentials to improve BPDES, polymer-free medicated as well as bare-metal chromium-bearing stents. In our opinion, the success of BPDES is inseparable with improved hemocompatibility of chromium-bearing stent platform.


### Acknowledgment

Fort Wayne Metals Research Products Corporation is gratefully acknowledged for providing Co-Cr alloy L-605 sample for the studies. We also are thankful to Mrs. Chandan Pulletikurthi from Florida International University, Miami, FL, USA for growing HUVEC cell cultures. Dr. Waseem Haider would also like to thank the US Army Research Office (W911NF-14-1-0100) for their support.


### Reference


1. B. Zuckerman, The Dual Antiplatelet Therapy (DAPT) Trial: An FDA Perspective, https://www.cardiac-safety.org/think-tanks/presentations-1/presentations-2009/4%20-%20Bram%20Zuckerman.pdf
2. R. Waksman, Drug-Eluting Stents: Will the Transformation to Bioabsorption Make Durable Polymers Obsolete, *Cardiovasc. Revasc. Med.*, 2013, **14**, p 69–70
3. S. Wood, Cordis Quits Coronary Stent Business, Dropping Cypher, Nevo DES. June 15, 2011 HeartWire, http://www.theheart.org/article/1238785.do
4. E.H. Christiansen, L.O. Jensen, P. Thayssen, H.H. Tilsted, L.R. Krusell, K.N. Hansen et al., Biolimus-Eluting Biodegradable Polymer-Coated Stent Versus Durable Polymer Coated Sirolimus-Eluting Stent in Unselected Patients Receiving Percutaneous Coronary Intervention (SORT OUT V): A Randomised Non-inferiority Trial, *Lancet*, 2013, **381**, p 661. doi:10.1016/S0140-6736(12)61962-X
5. P.C. Smits, S. Hofma, M. Togni, N. Vazquez, M. Valdes, V. Voudris et al., Abluminal Biodegradable Polymer Biolimus-Eluting Stent Versus Durable Polymer Everolimus-Eluting Stent (COMPARE II): A Randomised, Controlled, *Non-inferiority Trial. Lancet*, 2013, **381**, p 651. doi:10.1016/S0140-6736(12)61852-2
6. T. Tada, R.A. Byrne, T. Schuster, R. Cuni, H. Kitabata, K. Tiroch et al., Early Vascular Healing with Rapid Breakdown Biodegradable Polymer Sirolimus-Eluting Versus Durable Polymer Everolimus-Eluting Stents Assessed by Optical Coherence Tomography, *Cardiovasc Revasc Med*, 2013, **14**, p 84–89
7. L.V. Poperenko, M.F. Maitz, and M.V. Vinnichenko, Blood Compatibility Study of Chromium Oxide Films Deposited on Stainless Steel Surfaces by Magnetron Sputtering, *Funct. Mater.*, 2003, **10**(3), p 447–452
8. R. Rokicki, Apparatus and Method for Enhancing Electropolishing Using Magnetic Field. US Patent 7632390. http://www.freepatentsonline.com/7632390.html
9. T. Hryniewicz, K. Rokosz, and R. Rokicki, Electrochemical and XPS Studies of 316L Stainless Steel After Electropolishing in Magnetic Field, *Corros. Sci.*, 2008, **50**(9), p 2676–2681
10. R. Waksman, Will Biodegradable Polymers Replace Durable Polymers of the DES Technology, http://www.crtonline.org/flash.aspx?PAGE_ID=10249
11. S. Wood, Stent Pioneer Julio Palmaz Urges DES Makers to "Learn from Mistakes of the Past.(heart/wire)Interventional/Surgery October 27, 2009, http://www.theheart.org/article/1015869.do
12. B. O'Brien and W. Carroll, The Evolution of Cardiovascular Stent Material and Surfaces in Response to Clinical Drivers: A Review, *Acta Biomater.*, 2009, **5**, p 945–958
13. L. Raber, H. Kelbaek, M. Ostoijc, A. Baumbach, D. Heg, D. Tuller et al., Effect of Biolimus-Eluting Stents wit Biodegradable Polymers vs Bare-Metal Stents on Cardiovascular Events Among Patients with Acute Myocardial Infarction, *The COMFORTABLE AMI, Randomized Trial. JAMA.*, 2012, **308**(8), p 777–787. doi:10.1001/jama.2012.10065
14. I. De Scheerder, J. Sohier, K. Wang, E. Verbeken, X. Zhou, and L.E.T.A.L. Froyen, Metallic Surface Treatment Using Electrochemical Polishing Decreases Thrombogenicity and Neointimal Hyperplasia of Coronary Stents, *J. Interven. Cardiol.*, 2000, **13**(3), p 179–185
15. I. De Scheerder, J. Sohier, E. Verbeken, L. Froyen, and J. Van Humbeeck, Biocompatibility of Coronary Stent Material: Effect of Electrochemical Polishing, *Mat.-wiss.u. Werkstofftech.*, 2001, **32**, p 142–148
16. S.M. Slack, T.A. Horbett, The Vroman Effect, A Critical Review. Protein at Interfaces II, Book Chapter 8, p 112–128, ACS Symposium Series, Vol. 602
17. W. Norde and J. Lyklema, Protein Adsorption and Bacterial Adhesion to Solid Surfaces: A Physiochemical Approach, *Colloids Surf.*, 1989, **38**, p 1–13
18. A. Toscano and M. Santore, Fibrinogen Adsorption on Three Silica-Based Surfaces: Conformation and Kinetics, *Langmuir*, 2006, **22**, p 2588–2597
19. H. van Beusekom, P. Serruys, and W. van der Glessen, Coronary Stent Coatings, *Coron. Artery Dis.*, 1994, **5**, p 590–596
20. L. Lambrech, B. Young, and R. Stafford, The Influence of Preadsorbed Canine von Willebrand Factor, Fibrinonectin and Fibrinogen on Ex Vivo Artificial Surface-Induced Thrombosis, *Thromb. Res.*, 1986, **41**, p 99–117
21. S. Trigwell, G. Selvaduray, Effect of Surface Treatment on the Surface Characteristic of AISI 316L Stainless Steel, *Materials and Processes for Medical Devices Conference* November 14–16, 2005 Boston, MA, https://docs.google.com/viewer?a=v&q=cache:P9Sixn5uky0J:www.sjsu.edu/faculty/selvaduray/page/recent/316LStainlessSteel.pdf+&hl=en&gl=us&pid=bl&srcid=ADGEEShpMX8lSAjHC0j8yjy27dXdDM6JomxIfRarLodLf0TVwu1kFTcN5Klgtd9-qv-n-XNnv2rUh33FDV6jsC6TSl04R3kfTi-D05fvBPqmPMQU5sZ7shmN1ZD5Pb0bw-ye85zBxafk&sig=AHIEtbS7yNcQad74MhtQb4lFy_q_OOww7g
22. P. Barnabeu and A. Caprani, Influence of Surface-Charge on Adsorption of Fibrinogen and or Albumin on Rotating Disc Electrode of Platinum and Carbon, *Biomaterials*, 1990, **11**, p 258–264
23. J. Boilar, Ed., *The Chemistry of Coordination Compounds*, Reinhold Pbl, New York, 1966, p 448–471
24. T. Yoshioka, K. Tsuru, S. Hayakawa, and A. Osaka, Preparation of Alginic Acid Layers on Stainless-Steel Substrates for Biomedical Applications, *Biomaterials*, 2003, **24**(17), p 2889–2894
25. M. Lestellius, B. Liedberg, and P. Tengvall, In Vitro Plasma Protein Adsorption on ω-Functionalized Alkanethiolate Self-Assembled Monolayers, *Langmuir*, 1997, **13**(22), p 5900–5908
26. J. Lin and W. Chuang, Synthesis, Surface Characterization, and Platelet Reactivity Evaluation for the Self-Assembled Monolayer of Alkanethiol with Sulfonic Acid Functionality, *J. Biomed. Master Res.*, 2000, **51**(3), p 413–423
27. I.H. Bae, I.K. Park, D.S. Park, H. Lee, and M.H. Jeong, Thromboresistant and Endothelialization Effects of Dopamine-Mediated Heparin Coating on a Stent Material Surface, *J. Mater. Sci. Mater. Med.*, 2012, **23**, p 1259–1269
28. Y. Weng, J. Chen, Q. Tu, Q. Li, M. Maitz, and N. Huang, Biomimetic Modification of Metallic Cardiovascular Biomaterials: From Function Mimicking to Endothelialization In Vivo, *Interface Focus*, 2012, **2**, p 356–365
29. M. Martins, B. Ratner, and M. Barbosa, Protein Adsorption on Mixtures of Hydroxyl and Methyl-Terminated Alkanethiols Self-Assembled Monolayers on Gold Electrodes Studied by Chronopotentiometry, *Biomaterials*, 2003, **24**, p 3697–3706
30. B. Siravaman and R. Latour, The Adherence of Platelets to Adsorbed Albumin by Receptor-Mediated Recognition of Binding Sites Exposed by Adsorption-Induced Unfolding, *Biomaterials*, 2010, **31**(6), p 1036–1044